

Cobalt and copper pyridylmethylphosphonates with two- and three-dimensional structures and field-induced magnetic transitions

Ting-Hai Yang,^{a,c,d} Zhong-Sheng Cai^c, Fa-Nian Shi^{*b,d}, Li-Min Zheng^{*c}

^a School of Chemistry & Environmental Engineering, Jiangsu University of Technology, Changzhou 213001, P. R. China.

^b School of Science, Shenyang University of Technology, Shenyang 110870, P. R. China. E-mail: fshi96@foxmail.com.

^c State Key Laboratory of Coordination Chemistry, School of Chemistry & Chemical Engineering, Nanjing University, Nanjing 210093, P. R. China. E-mail: lmzheng@nju.edu.cn

^d Department of Chemistry, CICECO, University of Aveiro, 3810-193 Aveiro, Portugal.

Supporting Information

Contents

Figure S1: The layer structure of **1**.

Figure S2: The π - π stacking interaction in compound **1**

Figure S3: Layer topological structure of **1**

Figure S4: Topological structure of **2**

Figure S5: PXRD pattern for compound **1** with simulated one from single crystal data

Figure S6: PXRD pattern for compound **2** with simulated one from single crystal data

Figure S7: TG curves of complexes **1** and **2**

Figure S8: The χ_M^{-1} versus T plots for compound **1**

Figure S9: Temperature-dependent zero-field ac magnetic susceptibility for **1**

Figure S10: Differentiation of M versus H curve of **1**.

Figure S11: The χ_M^{-1} versus T plots for compound **2**

Figure S12: Temperature-dependent zero-field ac magnetic susceptibility for **2**

Figure S13: Differentiation of M versus H curve of **3**.

Table S1 Selected bond lengths [\AA] and angles [$^\circ$] for **1**

Table S2 Selected bond lengths [\AA] and angles [$^\circ$] for **2**

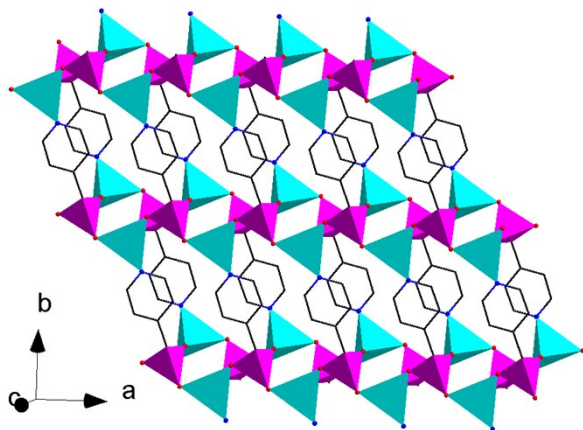


Figure S1 The layer structure of **1**. Cyan tetrahedron, CoNO_3 ; pink tetrahedron, PO_3C .

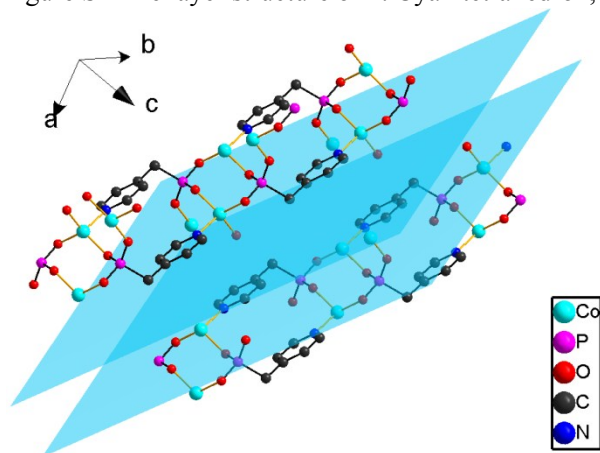


Figure S2 The π - π stacking interaction in compound **1**.

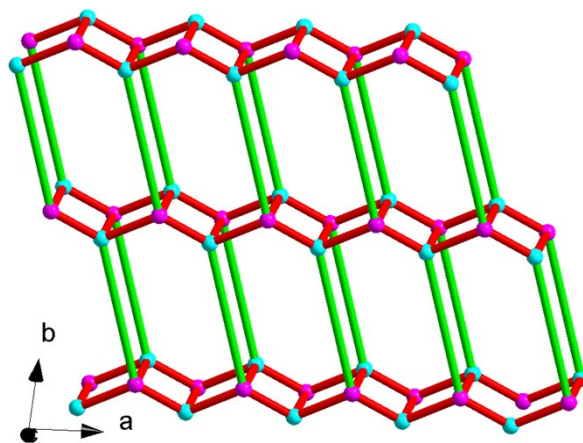


Figure S3 Layer topological structure of **1**. Cyan ball, Co atom; pink ball, P atom.

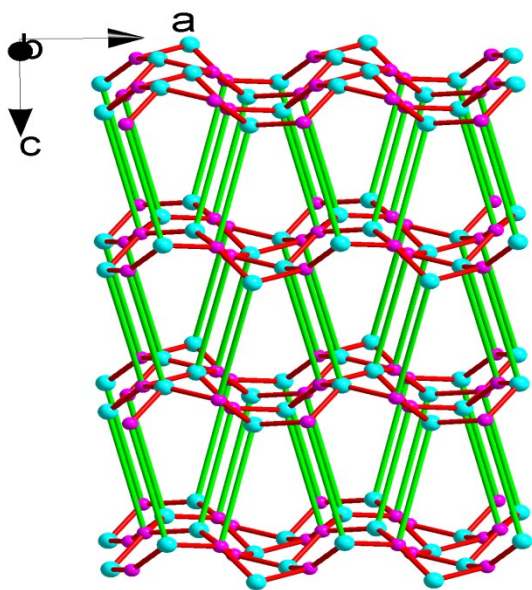


Figure S4 Topological structure of **2**. Cyan ball, Cu atom; pink ball, P atom.

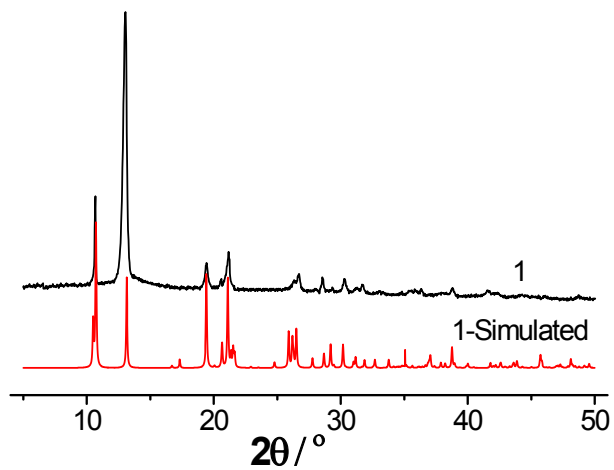


Figure S5 PXRD pattern for compound **1** with simulated one from single crystal data.

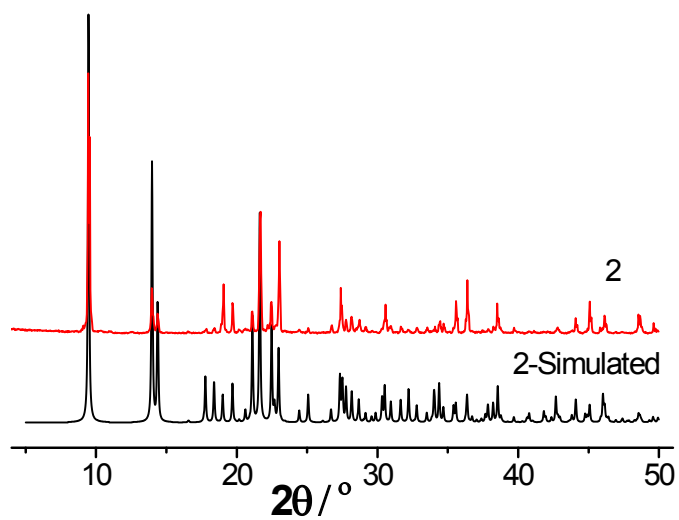


Figure S6 PXRD pattern for compound **2** with simulated one from single crystal data.

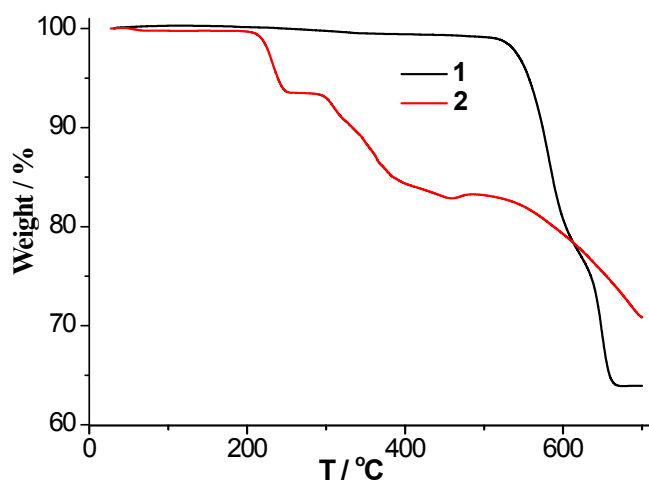


Figure S7 TG curves of complexes **1** and **2** (heating rate of 10 °Cmin⁻¹).

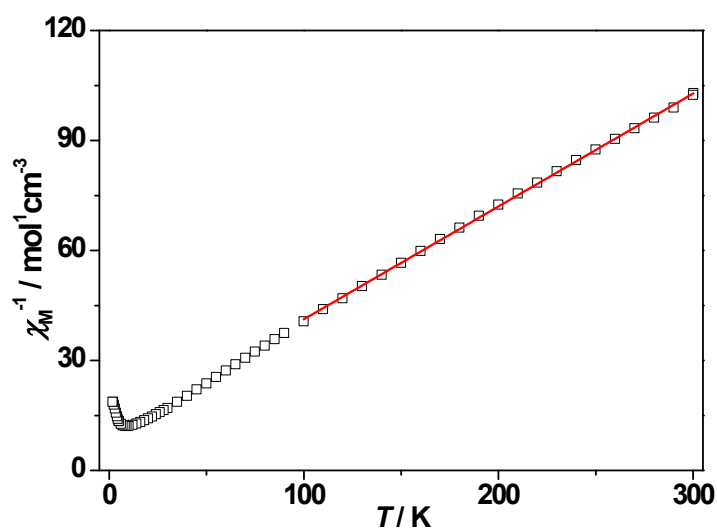


Figure S8 The χ_M^{-1} versus T plots for compound **1**.

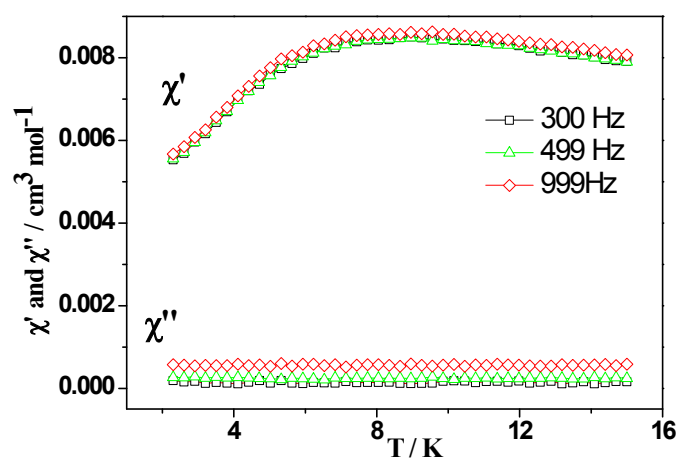


Figure S9 Temperature-dependent zero-field ac magnetic susceptibility for **1**.

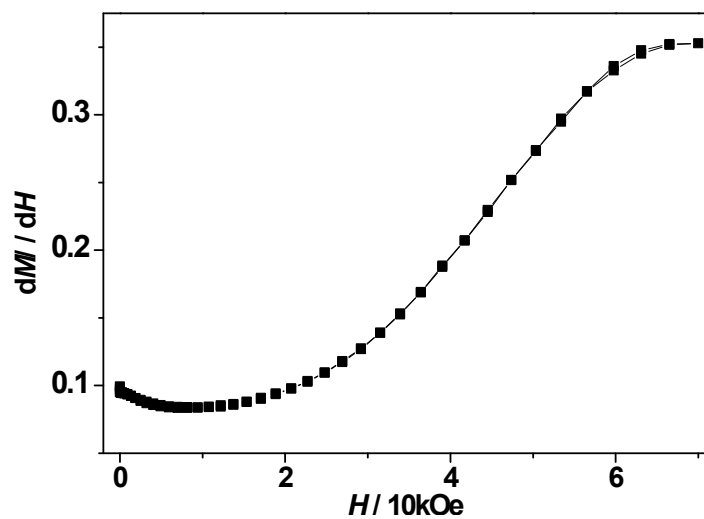


Figure S10 Differentiation of M versus H curve of **1**.

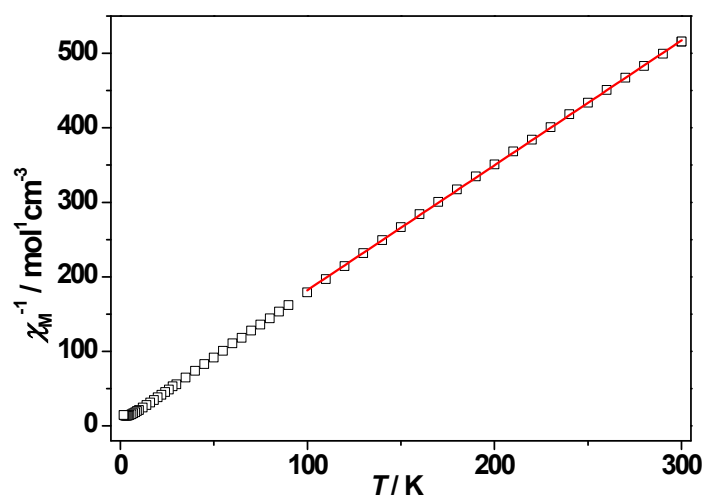


Figure S11 The χ_M^{-1} versus T plots for compound **2**.

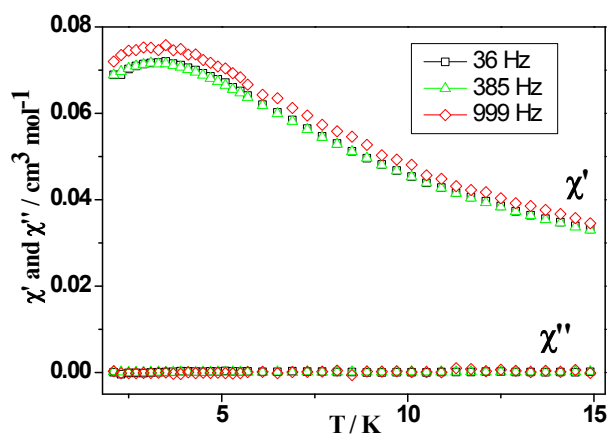


Figure S12 Temperature-dependent zero-field ac magnetic susceptibility for **2**.

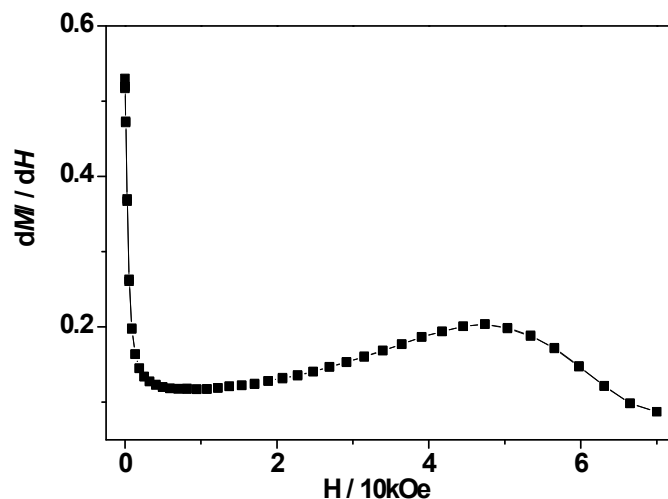


Figure S13 Differentiation of M versus H curve of **2**.

Table S1 Selected bond lengths [\AA] and angles [$^\circ$] for **1**.

Co(1)-O(2A)	1.937(2)	P(1)-O(1)	1.530(2)
Co(1)-O(1)	1.974(2)	P(1)-O(2)	1.523(2)
Co(1)-O(3B)	1.944(2)	P(1)-O(3)	1.519(2)
Co(1)-N(1C)	2.049(3)	P(1)-C(1)	1.812(3)
O(2A)-Co(1)-O(3B)	120.64(10)	O(2A)-Co(1)-O(1)	115.65(10)
O(3B)-Co(1)-O(1)	107.94(9)	O(2A)-Co(1)-N(1C)	97.60(10)
O(3B)-Co(1)-N(1C)	109.50(10)	O(1)-Co(1)-N(1C)	103.49(10)

Symmerty codes : A: $-x+1,-y,-z+1$; B: $x+1,y,z$; C: $x-1,y,z$.

Table S2 Selected bond lengths [\AA] and angles [$^\circ$] for **2**.

Cu(1)-O(1)	1.9579(14)	Cu(1)-N(1C)	2.2320(17)
Cu(1)-O(2B)	1.9938(14)	P(1)-O(1)	1.5181(13)
Cu(1)-O(3A)	1.9869(14)	P(1)-O(2)	1.5326(14)
Cu(1)-O(4)	1.9755(14)	P(1)-O(3)	1.5248(15)
O(1)-Cu(1)-O(3A)	90.26(6)	O(1)-Cu(1)-O(2B)	89.43(6)
O(4)-Cu(1)-O(3A)	86.61(6)	O(4)-Cu(1)-O(2B)	91.22(6)
O(1)-Cu(1)-N(1C)	95.86(6)	O(4)-Cu(1)-N(1C)	92.93(6)
O(3A)-Cu(1)-N(1C)	90.01(6)	O(2B)-Cu(1)-N(1C)	105.57(6)

Symmerty codes : A: $x+1/2,y,-z+3/2$; B: $-x,y-1/2,-z+3/2$; C: $x,-y+3/2,z+1/2$.